Journal of Hydrology 450–451 (2012) 117–133

Contents lists available at SciVerse ScienceDirect

Journal of Hydrology

journal homepage: www.elsevier.com/locate/jhydrol

The role of bedrock groundwater in rainfall–runoff response at hillslope and catchment scales

C.P. Gabrielli [a,*], J.J. McDonnell [b], W.T. Jarvis [c,d]

[a] Department of Forest Engineering, Resources and Management, Oregon State University, Corvallis, OR 97331, USA
[b] Global Institute for Water Security, National Hydrology Research Centre, University of Saskatchewan, 11 Innovation Boulevard, Saskatoon, SK, Canada S7N 3H5
[c] Institute for Water and Watersheds, Oregon State University, Corvallis, OR 97331, USA
[d] Department of Geosciences, Oregon State University, Corvallis, OR 97331, USA

ARTICLE INFO

Article history:
Received 17 November 2011
Received in revised form 2 May 2012
Accepted 9 May 2012
Available online 18 May 2012
This manuscript was handled by Philippe Baveye, Editor-in-Chief, with the assistance of M. Todd Walter, Associate Editor

Keywords:
Hillslope hydrology
Rainfall runoff
Bedrock groundwater
Stormflow

SUMMARY

Bedrock groundwater dynamics in headwater catchments are poorly understood and poorly characterized. Direct hydrometric measurements have been limited due to the logistical challenges associated with drilling through hard rock in steep, remote and often roadless terrain. We used a new portable bedrock drilling system to explore bedrock groundwater dynamics aimed at quantifying bedrock groundwater contributions to hillslope flow and catchment runoff. We present results from the Maimai M8 research catchment in New Zealand and Watershed 10 (WS10) at the H.J. Andrews Experimental Forest in Oregon, USA. Analysis of bedrock groundwater at Maimai, through a range of flow conditions, revealed that the bedrock water table remained below the soil–bedrock interface, indicating that the bedrock aquifer has minimal direct contributions to event-based hillslope runoff. However, the bedrock water table did respond significantly to storm events indicating that there is a direct connection between hillslope processes and the underlying bedrock aquifer. WS10 groundwater dynamics were dominated by fracture flow. A highly fractured and transmissive zone within the upper one meter of bedrock conducted rapid lateral subsurface stormflow and lateral discharge. The interaction of subsurface stormflow with bedrock storage directly influenced the measured hillslope response, solute transport and computed mean residence time. This research reveals bedrock groundwater to be an extremely dynamic component of the hillslope hydrological system and our comparative analysis illustrates the potential range of hydrological and geological controls on runoff generation in headwater catchments.

1. Introduction

Process understanding of the rainfall–runoff response of steep hillslopes and headwater catchments has evolved greatly since the foundational work of Hursh (1936). Early reviews (Dunne, 1978) and more recent reviews (Bonell, 1998; Bachmair and Weiler, 2011) have chronicled the development of concepts on rapid subsurface stormflow development and the integration of individual hillslope responses that create the integrated catchment response. Despite extensive research revealing dominant processes in different environments, the majority of the work to date has focused exclusively on lateral flow in the soil mantle (Buttle, 1998; Hewlett and Hibbert, 1967; McDonnell, 1990; Tsuboyama et al., 1994).

Despite a largely soil-centric view of hillslope hydrology, early work by Wilson and Dietrich (1987) in a zero order basin in California showed the potentially significant hydrologic influence of underlying bedrock in rainfall–runoff delivery at the hillslope scale. They found that stormflow followed fracture pathways within the shallow weathered bedrock and interacted with the overlying colluvium when flows were forced upwards by more competent bedrock, creating zones of transient saturation. Later work at the Coos Bay Oregon site by Montgomery et al. (1997) and Anderson et al. (1997) also noted subsurface flow paths that traversed the soil and bedrock zones in steep unchanneled slopes. Water exfiltrating from the bedrock during storm events and sprinkling experiments produced perched transient water tables at the soil–bedrock interface that influenced directly, subsurface stormflow and slope instability. Additionally, their bromide tracer injections showed rapid movement of bedrock flow to the catchment outlet identifying the importance of bedrock flow paths for hillslope-to-catchment integration. More recently, Kosugi et al. (2008), building upon other important work in Japan (Katsuyama et al., 2005; Onda et al., 2001; Uchida et al., 2003), showed the importance of bedrock groundwater in a granitic catchment in Central Japan. They found that transient saturation at the soil bedrock interface was connected to the rise and fall of deeper bedrock

* Corresponding author. Tel.: +1 603 568 6187.
E-mail addresses: Chris.Gabrielli@gmail.com (C.P. Gabrielli), jeff.mcdonnell@orst.edu (J.J. McDonnell), todd.jarvis@oregonstate.edu (W.T. Jarvis).

0022-1694/$ - see front matter © 2012 Elsevier B.V. All rights reserved.
http://dx.doi.org/10.1016/j.jhydrol.2012.05.023

groundwater that ultimately influenced the chemical, spatial and temporal characteristics of subsurface water movement into the stream channel.

In some bedrock aquifers, fracture flow is the key feature controlling bedrock groundwater contributions to hillslope flow and catchment runoff response. Fracture flow through bedrock is controlled by fracture network density, geometry and connectivity (Banks et al., 2009) and can be extremely complex and heterogeneous. Fracture zones separated by competent bedrock may create compartmentalized aquifers, while faulting, weathering and other large scale geologic processes may help induce connectivity between fracture pathways (Dietrich et al., 2005). Haria and Shand (2004) found complex flow processes at depth-specific horizons in fractured bedrock in the riparian and lower hillslope region of the Hafren catchment in Plynlimon, Wales. They observed that the dual-porosity environment of fractured bedrock promoted rapid storm response and minimal storage on a storm event time scale.

Despite growing awareness of the potential significance of bedrock groundwater at hillslope and catchment scales, there still remains a very limited number of studies that have monitored hillslope groundwater in competent and fractured bedrock (McDonnell and Tanaka, 2001). Access remains the key logistical hurdle limiting studies in characteristically steep, unstable, and often roadless headwater terrain. Where access has been limited, many studies have inferred catchment groundwater dynamics through intensive studies of spring discharge, rather than direct measurements taken within the bedrock itself (Iwagami et al., 2010; Katsuyama et al., 2005; Uchida et al., 2003). While useful, the black box nature of spring studies limit our ability to mechanistically assess the dynamics of internal bedrock groundwater and its connection to hillslope processes in the soil mantle. Indeed, in hillslope and catchment hydrology we struggle to know the general involvement, if at all, of bedrock groundwater in forming saturation at the soil–bedrock interface where large anisotropy and rapid generation of lateral subsurface stormflow has been widely observed (Weiler et al., 2006). We lack, particularly at previously well-monitored and well-documented sites, an understanding of how bedrock groundwater couples to rapid event runoff generation and flow sustenance in the stream between events.

Here we tackle fundamental questions of bedrock groundwater contributions through a comparative analysis of two well-studied hillslopes. We capitalize on a new portable drill system developed by Gabrielli and McDonnell (2011). Capable of drilling wells up to 10 m deep in a variety of geological formations (colluvium, saprolite, competent and fractured bedrock), this drill system can be carried into field sites, previously inaccessible by standard truck mounted drill rigs. It thus presents an inexpensive solution to directly access bedrock groundwater in the headwaters. Few, if any, bedrock groundwater studies to date have been conducted at sites with rich histories of hillslope experimental studies.

We base our work on the null hypothesis that bedrock groundwater does not contribute materially to hillslope or catchment runoff dynamics. We then investigate how bedrock structure affects hillslope response to storm events at the M8 experimental hillslope and catchment at Maimai in New Zealand, and the Watershed 10 experimental hillslope and catchment at the H.J. Andrews in the Cascade Range in Oregon, USA. Beven (2006) has characterized both sites as benchmarks in the field: Maimai for work by Mosley (1979) and his 'fundamental insights into this quintessential, wet, steep, humid, forested catchment' (Beven, 2006, p. 336); the H.J. Andrews for work by Harr (1977) and his 'characterization of subsurface flow processes' and their link to catchment scale rainfall–runoff dynamics (Beven, 2006, p. 266).

Here we build upon these and the many subsequent studies at Maimai and H.J. Andrews to answer the following questions in relation to the role of bedrock groundwater in rainfall–runoff response at hillslope and catchment scales:

A. How do hydrogeological features and the structure of bedrock influence bedrock groundwater movement at the hillslope scale?
B. How does bedrock groundwater react to storm events?
C. Does bedrock groundwater contribute directly to hillslope discharge through exfiltration at the soil–bedrock interface?

We address these questions by combining standard hydrometric approaches that include wells, hillslope trenches and gauging stations, with the new Gabrielli and McDonnell (2011) drilling system and stable isotope tracer analysis of storm event streamflow, hillslope trench water and bedrock groundwater. We targeted nine and 16 week field campaigns during the wet season at the Maimai and H.J. Andrews, respectively.

2. Study sites

Two well-established benchmark experimental hillslopes and catchments were investigated: Watershed M8 (M8) at the Maimai in New Zealand and watershed 10 (WS10) at the H.J. Andrews in Oregon, USA. These watersheds appear nearly identical in many respects including size, physical hillslope characteristics and rainfall–runoff characteristics (Table 1). They differ significantly, however, in their underlying bedrock geology. WS10 is dominated by layers of fractured pyroclastic tuff and breccias (Swanson and James, 1975). M8 is underlain by a firmly-compacted conglomerate with little or no fracturing (O'Loughlin et al., 2002). Additionally,

Table 1
M8 and WS10 hillslope and catchment physical, meteorological and process characteristics. *Source*: Sayama and McDonnell (2009) as summarized from primary literature from the two sites.

Characteristic	M8, Maimai	WS10, H.J. Andrews
Size (ha)	3.8[a]	10.2
Slope angle (°)	34	29
Slope length (m)	<300	<200
Local relief (m)	100–150	60–130
Soil type	Silt loams	Clay loams
Mean soil depth	0.7 (0.5–1.8)	3.0 (1.5–4.2)
Soil infiltration capacity ($mm\ h^{-1}$)	6100	>5000
Soil Ksat ($mm\ h^{-1}$)	250	275
Bedrock type	Moderately weathered Pleistocene conglomerate	Weathered and fractured pyroclastic Tuff and Breccias
Vegetation cover	Mixed evergreen forest	Second growth douglas-fir
Avg. annual rainfall (mm)	2600	2350
Seasonality	Year round (event every ~3 days)	80% Falls between October and April
Catchment runoff ratio (%)	60	56
Hillslope runoff ratio (%)	13	80
Runoff characteristics	Very responsive	Very responsive
Pre-event water ratio	>70	75–80
Stream water MRT	4 months	1.2 years
Bedrock porosity characteristics	Porous media	Dual porosity

[a] M8 catchment size is calculated from the area upstream of a previously destroyed gauging weir located 100 m upstream of the instrumented hillslope we studied and therefore, actual area including the instrumented hillslope is slightly larger.

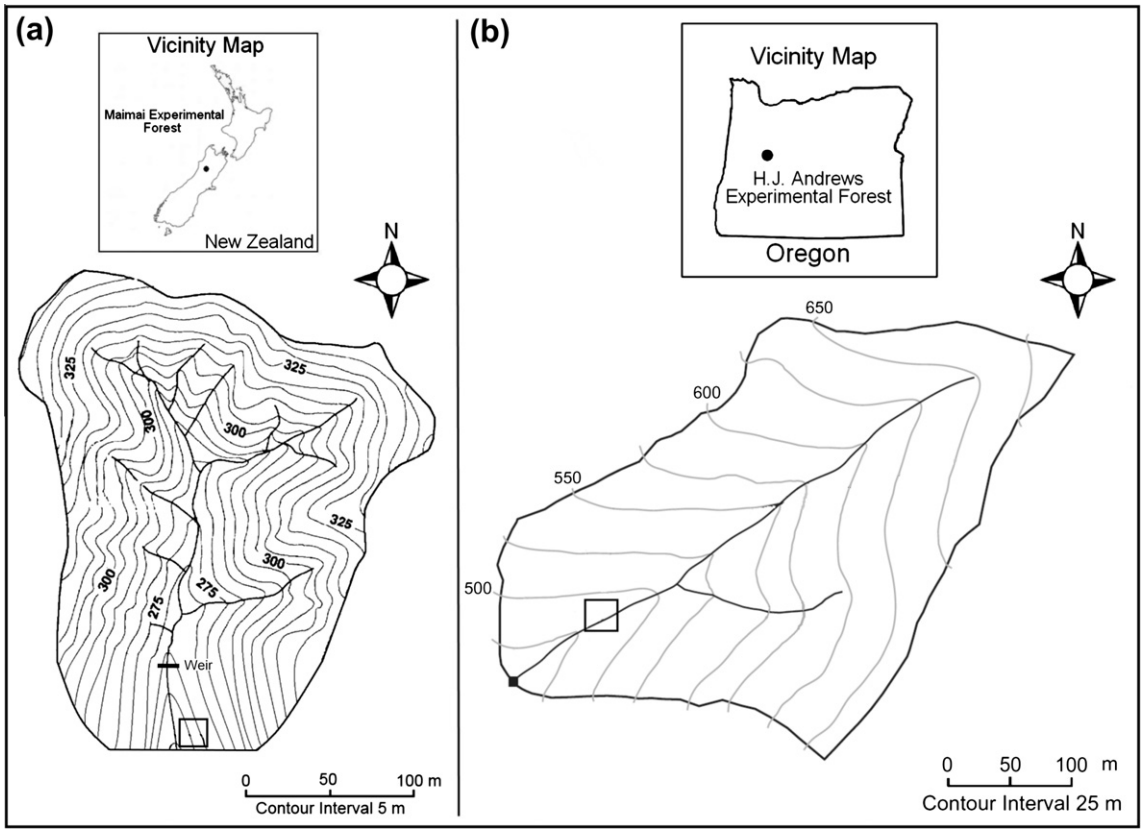

Fig. 1. Vicinity and catchment map for (a) the M8 catchment at the Maimai Experimental Forest and (b) the WS10 catchment at the HJ Andrews Experimental Forest. Black squares represent the approximate location of the instrumented hillslopes.

despite similar catchment runoff ratios these sites have very contrasting hillslope runoff ratios as well as differing catchment mean residence times, suggesting their hillslopes may shed water through different mechanisms based at least partially upon differing bedrock permeability architecture.

2.1. Maimai M8

The M8 study site shown in Fig. 1a, is a 3.8 ha watershed located on the West Coast of the South Island of New Zealand (42.1° S, 171.8° E). McGlynn et al. (2002) provide a complete description as well as a historical review of the research conducted within the catchment. Our description is based on their review. Low-intensity, long-duration storms produce an average annual rainfall of 2600 mm (Woods and Rowe, 1996). Monthly rainfall is distributed evenly between April and December, with slightly drier conditions existing between January and March. The catchment is very responsive and runoff ratios (catchment discharge/rainfall) are approximately 60% annually (Rowe and Pearce, 1994). Slopes are short (<300 m) and steep (mostly above 35°) with a local relief of 100 m.

Hillslope soils are characterized as stony podzolized yellow brown earth (Blackball hill soils). Average soil profile is 0.60 m (range 0.25–1.30 m); soils are deeper hollows and at the toe of slopes where material has accumulated and shallower near ridgelines and spurs (Woods and Rowe, 1996). Hydraulic conductivity of the mineral soils range from 5 to 300 mm h^{-1} and mean soil porosity is 45% (McDonnell, 1990). High annual rainfall and high storm frequency (average time between storms ~3 days) results in a soil profile that remains within 10% of saturation during most of the year (Mosley, 1979). Underlying the soils is a moderately weathered, firmly compacted, Early Pleistocene conglomerate known as the Old Man Gravel formation. The conglomerate is comprised of clasts of sandstone, schist and granite in a clay–sand matrix (Rowe et al., 1994) and is considered poorly permeable with estimated seepage losses of 100 mm yr^{-1} (Rowe and Pearce, 1994). More recent work by Graham et al. (2010b) has shown that Old Man Gravel saturated hydraulic conductivity (Ksat) may be on the order of 1–3 mm h^{-1}, implying a larger annual and within-storm loss to bedrock.

The gauged hillslope at M8 has been the site of many studies completed over the past 20 years (McDonnell, 1990; McDonnell et al., 1998; Woods and Rowe, 1996), as well as many recent studies (Graham and McDonnell, 2010; Graham et al., 2010b; McGlynn et al., 2004). First instrumented by Woods and Rowe (1996), this planar hillslope has maximum slope lengths of 50 m and slope angles greater than 35°. A 60 m long trench originally built by Woods and Rowe (1996) is installed to the bedrock surface to collect subsurface flow from the hillslope. The trench is separated into 1.7 m sections, each of which routes flow to individual recording tipping buckets. Graham et al. (2010b) removed four trench sections and excavated the soil down to bedrock across an area of approximately 50 m^2 just upslope of the trench sections.

2.2. H.J. Andrews WS10

WS10 is located at the H.J. Andrews Experimental Forest (HJA) and is part of a Long Term Ecological Research program in the west central Cascade Mountains of Oregon, USA (44.2° N, 122.25° W). McGuire et al. (2007) synthesized past research at the site, as well as a full description of site characteristics. Our description is based on their review. Mild wet winters and warm dry summers characterize the Mediterranean climate at WS10. Annual mean precipitation is 2350 mm (averaged from 1990 to 2002) with 80% falling

between October and April. A wet-up period exists from the start of each water year through December, after which the catchment remains in a very wet and highly responsive state. Long duration, low to moderate intensity frontal storms characterize the rainfall regime. On average, 56% (28–76%) of rainfall becomes runoff (McGuire et al., 2005). Summer baseflows are approximately 0.2 L s^{-1} (<0.01 mm h^{-1}) and archetypal winter storms reach peak flows of approximately 40 L s^{-1} (1.4 mm h^{-1}) (McGuire and McDonnell, 2010). Transient snow accumulation is common, but rarely persists more than 1–2 weeks and generally melts within 1–2 days (Mazurkiewicz et al., 2008).

The 10.2 ha catchment ranges in elevation from 473 m at the gauged flume to 680 m at ridge top (Fig. 1b). The terrain is characterized by short (<200 m), steep slopes ranging from 30° to greater than 45°. Periodic debris flows (most recently in 1986 and 1996) have scoured the lower 60% of the stream channel to bedrock and removed the riparian zone, resulting in a catchment dominated by hillslope runoff with very little riparian volume or storage. Well-defined seeps flowing from the base of the hillslopes into the stream channel have been identified and are known to sustain a substantial portion of the summer low flow (Harr, 1977; Triska et al., 1984). Swanson and James (1975) and Harr (1977) established the origins of these hillslope seeps as either localized saturated zones controlled by the topographic convergence of the underlying bedrock or the presence of vertical andesitic dykes approximately 5 m wide that are located within the basin.

The gauged hillslope at WS10 has been the site of many benchmark studies completed in the 1970s (Harr, 1977; Harr and Ranken, 1972; Sollins et al., 1980; Sollins and McCorison, 1981), followed by many recent studies (McGuire and McDonnell, 2010; McGuire et al., 2005, 2007; van Verseveld et al., 2009). The hillslope study area is located on the south aspect of WS10, 91 m upstream from the stream gauging station (Fig. 1a) (McGuire and McDonnell, 2010). The average slope angle is 37°, ranging from 27° near the ridge to 48° where it intersects the stream. The slope is slightly convex along its 125 m length from stream to ridgeline. The hillslope comprises of residual and colluvial clay loam soils derived from andesitic tuffs (30%) and coarse breccias (70%) that formed as a result of ashfall and pyroclastic flows from the Oligocene–Early Miocene period (James, 1977; Swanson and James, 1975). Well-aggregated surface soils give way to more massive blocky structure and less aggregation at depths of 0.7–1.1 m (Harr, 1977). Average soil depth is approximately 3 m. Moderately to highly weathered parent material (saprolite) ranges in thickness from 0 to 7 m and emerges approximately 30 m upslope from the stream channel and extends to ridgeline (Harr and McCorison, 1979; Sollins and McCorison, 1981). Across the first 30 m of hillslope, before the emergence of the saprolite layer, the soil mantle sits directly over ~1 m of highly-fractured, slightly-weathered bedrock.

3. Methods

We combined physical, hydrogeologic, and environmental tracer measurements at each study site to characterize the bedrock groundwater system. A new portable bedrock-drilling system (Gabrielli and McDonnell, 2011) was utilized to drill boreholes into bedrock at each hillslope. Monitoring of the water table during and between precipitation events, as well as geologic information gained through bedrock core recovery provided the hydraulic and hydrogeologic data to characterize dynamics of the shallow bedrock groundwater response during storm events. Core samples and outcrop samples provided data for the geological interpretation of lithographic layers within each hillslope. When possible, well logs were constructed for each borehole using cores and drilling observations. These logs provided a visual reference to the geological structure of each borehole and the larger surrounding hillslope.

Sampling of rain, stream, trench and bedrock well water was conducted for a single precipitation event at each study site to evaluate isotopic composition of $\delta^{18}O$ and $\delta^{2}H$ and identify flow paths and mixing processes within the hillslope. These featured storms occurred within the 9 and 16 week field campaign at each site (M8 and WS10, respectively), and focused on each catchment's wet season with the objective of capturing each hillslope in its wettest state, and hence, the most likely time for bedrock groundwater involvement in lateral subsurface stormflow.

3.1. Maimai M8

We located our study on the same instrumented hillslope as Graham et al. (2010b) and Woods and Rowe (1996). We installed five bedrock wells, labeled 1–5, along a transect perpendicular to the stream channel starting 15 m from the stream channel and spaced at approximately 6 m intervals (Fig. 2a). The wells ranged in depth from 3.4 to 5.5 m into the bedrock (Table 2). The first two wells in the transect were located within the region cleared of soil by Graham et al. (2010b), while the wells further upslope were installed through the overlying soil mantle. A sixth well (3a) was drilled at the same elevation as Well 3 but offset 5 m upstream of the transect.

Well installation started by drilling a 0.10 m diameter hole through the colluvial layer with a hand auger. PVC casing was inserted down to bedrock to prevent collapse of the surrounding soil. The portable bedrock drilling system design by Gabrielli and McDonnell (2011) was then used to drill through the Old Man Gravel. Each well was drilled to 64 mm in diameter for the initial 0.6 m of depth, after which, additional drilling was done at 38 mm in diameter. Thirty mm diameter PVC, screened along its entire length, was used to case each borehole. A plastic collar was placed around the outside of the PVC casing at the depth where the borehole transitioned from larger to smaller diameter. Bentonite was then backfilled into the annulus between the 63 mm borehole and the casing, effectively creating a watertight seal that extended from 0.6 m into the bedrock up to the soil surface. This seal ensured that soil water could not infiltrate into the well and contaminate the bedrock groundwater. Wells were instrumented with an unvented Onset™ U20 pressure transducer capable of measuring water depths to 9 m within ±5 mm. Ten minute recording intervals were used. A similar pressure transducer was placed in a research facility ~200 m from the hillslope to record barometric pressure, which was used to convert absolute pressure to water depth measurements in each well. Data were collected over a period of 65 days between 1 July, 2010 and 3 September, 2010.

Slug and pumping tests were conducted for each well to help characterize the hydraulic properties of the bedrock. A hand operated peristaltic pump was used for pump tests at a rate of 0.25 L min^{-1} for all wells. Well 1 was pumped for 60 min, while all other wells were only pumped for 10 min due to extremely slow recharge. Slug tests were conducted by injecting instantaneously, 4 L of water into each well and recording the falling head using an Onset™ U20 pressure transducer recording water height every 10 s. Hydraulic conductivity (Ksat) was calculated using the Dagan (1978) method.

Two 1.7 m sections of the hillslope trench, initially installed by Woods and Rowe (1996), were reestablished and equipped with 1 L tipping buckets to record hillslope runoff. Trench sections 15 and 16 were used, and a description of the trench design can be found in Woods and Rowe (1996). An Ota Keiki tipping bucket rain gauge calibrated at 0.2 mm per tip recorded precipitation at

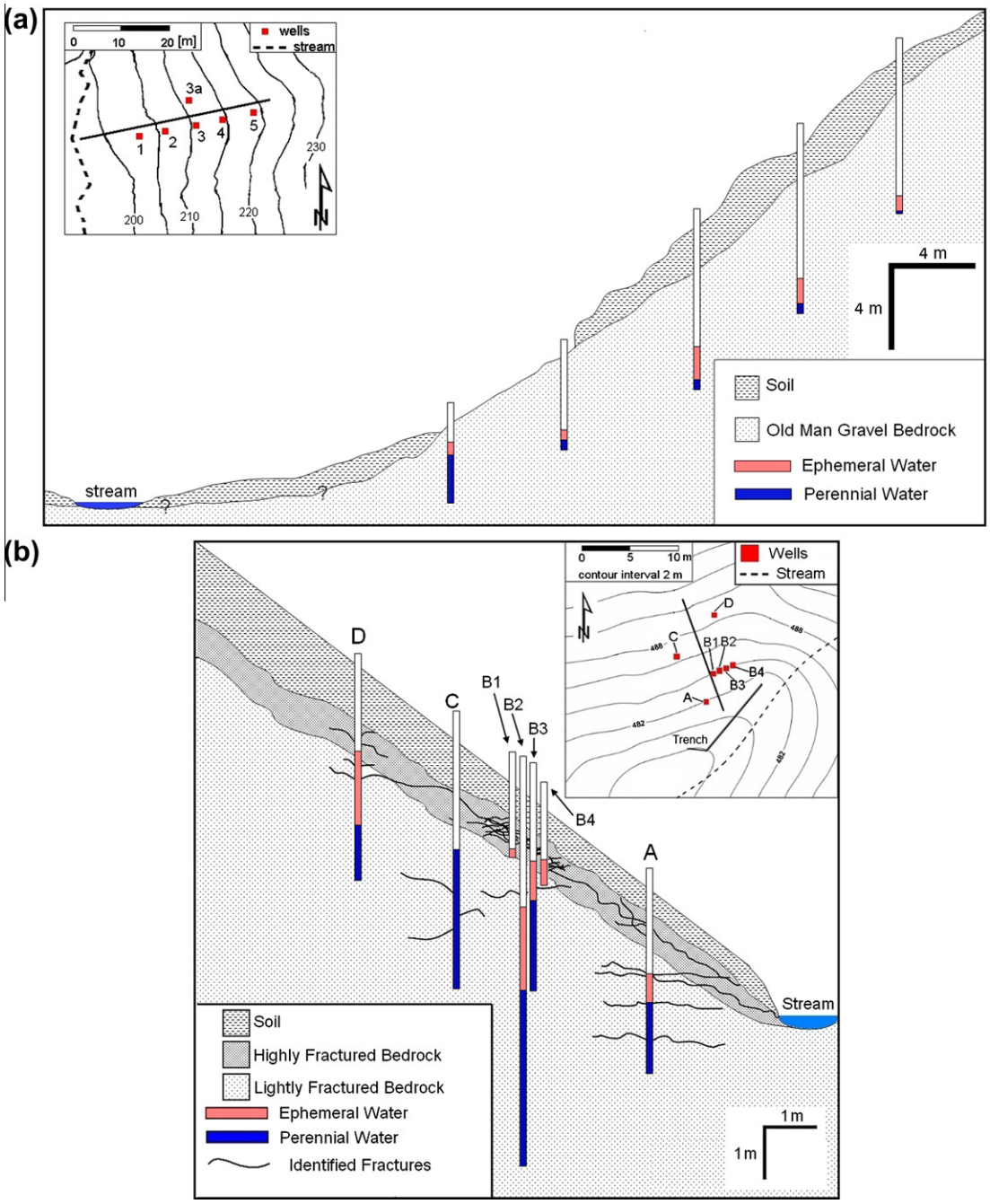

Fig. 2. Profile of instrumented hillslopes at M8 (a) and WS10 (b) showing well depths, water level dynamics through the duration of the study period and geology. Here we define perennial water as that water was present in the well through the duration of the study period, while ephemeral water existed only during precipitation events. The inset maps show plan view of well location and transect line of profile. Core samples from wells were used to define the geological structure shown and to locate the water table in the bedrock. Note the missing soil in (a) due to the excavation work by Graham et al. (2010a,b).

ground level 5 m from the trenched hillslope (J. Payne, personal communication, July, 2010). Stream discharge was measured at a 90° V-notch weir installed 20 m upstream of the gauged hillslope. Two capacitance rods (Tru Track, Inc., model WTDL 8000) recorded stage height on 10 min intervals. We note here that the catchment boundary for M8 shown in Fig 1 is somewhat larger than reported in previous (pre-1990) studies. This is due to a weir replacement following a 1988 debris flow that destroyed the original weir for the then, 3.8 ha catchment. The new weir was constructed ~100 m downstream, as shown in Fig 1, resulting in a slightly expanded catchment area (an area that ultimately is unknown given the poor DEM information available). We computed runoff depths based on the original 3.8 ha area estimate and did not use calculated runoff depths for anything beyond timing analysis. Runoff depth comparisons used later in the paper rely on pre-1988 measurements of M8 flow.

A single 36 mm rainfall event was sampled for $\delta^{18}O$ and $\delta^{2}H$ isotopic composition. Rainfall was sampled hourly, independent of sample volume. Runoff and trenchflow were sampled hourly from the onset of the event until 3 h past the peak of the hydrograph and then every 2–4 h through the recession for a total sampling period of 47 h. Stream water and Wells 1, 2, 3, and 5 were sampled during each sampling period. High frequency trench and rain water samples were collected hourly for the duration of measurable water.

Table 2
Well characteristics at M8, Maimai and WS10, H.J. Andrews.

Well	Distance from stream channel (m)	Depth into bedrock (m)	Screened interval (m)	Mid-screen depth (m)	*K*sat (mm/d)	Fracture density, fractures per m (upper most m/lower bedrock)	Average depth to water table[a] (m)	Average water table response to precip[b] (mm/mm)	Spearman's rank (Rho)
M8, Maimai									
1	13.7	3.4	2.5	2.2	3.12	–	1.49 ± 0.03	0.91 ± 0.21	0.72
2	18.9	4.0	3.1	2.5	0.0012	–	3.61 ± 0.06	1.69 ± 1.35	0.45
3	23.4	5.3	4.4	3.1	0.0009	–	4.38 ± 0.34	6.66 ± 6.55	0.24
3a	24.6	4.9	4.0	2.9	0.0023	–	4.08 ± 0.31	4.58 ± 5.98	–
4	28.0	5.5	4.6	3.2	0.0005	–	4.61 ± 0.26	3.59 ± 2.68	0.28
5	32.5	5.2	4.3	3.0	0.0003	–	4.86 ± 0.16	1.59 ± 1.00	0.24
WS10, H.J. Andrews									
A	3.2	3.4	3.4	1.7	–	26/6	1.48 ± 0.18	8.59 ± 5.22	0.63
B1	4.6	0.9	0.7	0.6	–	28/–	0.81 ± 0.01	7.23 ± 5.71	0.91
B2	4.6	3.5	2.0	2.5	–	29/7	1.45 ± 0.09	1.92 ± 1.59	0.43
B3	4.6	7.5	3.0	6.0	–	25/4	3.18 ± 0.27	13.94 ± 11.82	0.58
B4	4.6	1.0	0.3	0.9	–	27/–	0.91 ± 0.01	–	–
C	6.2	4.6	2.0	3.6	–	18/9	1.49 ± 0.03	1.28 ± 0.72	0.48
D	6.4	3.8	2.2	2.7	–	21/6	1.91 ± 0.62	21.80 ± 10.88	0.88

[a] Average calculated over entire data collection time period for each site.
[b] Average based on storm events greater than 20 mm total precipitation. Water table response for each storm was calculated as the difference between pre-storm and peak water table level.

Isotope analysis was conducted using an LGR liquid water isotope analyzer (LWIA-24d).

Multiple bedrock samples of approximately 0.15 × 0.15 × 0.15 m in size were removed from the open bedrock surface using a metal pick and brought back to the lab for measurement of porosity. Samples were oven dried at 60 °C until weight loss was negligible. The bedrock samples were then cooled to room temperature before being submerged in DI water at room temperature for 4 days. Saturated and oven-dry weights, as well as volumes calculated from displaced water volumes, were used to determine approximate porosity.

3.2. H.J. Andrews WS10

Seven bedrock wells (A, B1, B2, B3, B4, C and D) were installed into the hillslope bedrock in a network configuration (Fig. 1b). Wells B1–B4 were drilled as a cluster to investigate vertical head gradients within the bedrock. Wells were spaced between 2 and 7 m from the stream channel and depths ranged from 0.9 to 7.5 m into bedrock (Table 2). Overlying soil depth was between 0 and 1.5 m. Bedrock cores were recovered from each borehole and used to construct well logs for geotechnical information. Difficulties with sealing the wells to prevent soil water from contaminating the bedrock groundwater required the use of well-packers instead of the sealing method used at M8. Inflatable well packers are commonly used in these settings by lowering the device into a borehole to a specific depth; a rubber bladder is then inflated producing a watertight seal against the wall of the borehole (J. Istok, personal communication, October 2010). Small air leaks can sometimes cause the bladders to deflate over long periods of time. Boreholes were also backfilled with bentonite up to the soil surface to ensure a waterproof seal. Unvented Onset™ U20 pressure transducers were placed below the inflatable packers to measure water depth. Fracture networks and borehole depths were used to determine the exact location of packer placement for each well and allowed for the isolation of specific fracture regions. A venting tube was placed from the surface through the well packer to provide atmospheric pressure conditions within each well. Data were collected over a period of 112 days from 12 December, 2010 to 1 April, 2011. Barometric pressure data, collected at the H.J. Andrews Headquarters 1 km away, was used to convert absolute pressure to water depth.

The hillslope includes a 10 m long trench installed to bedrock at the intersection of the hillslope and stream channel. Hillslope runoff was directed through a 15° V-notch weir and two Tru-Trac™ capacitance rods recorded stage height at 10 min intervals. Stream discharge was measured at a gauging station 90 m downstream of the hillslope, and rainfall data was collected 1 km away at the H.J. Andrews Headquarters.

A single 34 mm rainfall event was sampled for $\delta^{18}O$ and $\delta^{2}H$ isotopic composition. 50 mL samples were collected on an hourly basis from the onset of the event until 3 h after the hydrograph peak, after which samples were taken every 2–4 h through the recession for a total sampling period of 42 h. Water from Wells A and D, the trench and stream, were collected during each sampling round while the remainder of the wells were sampled as they wetted up through the event and for the duration of measurable water. Rainfall samples were collected on an hourly basis for the duration of the event. Isotope analysis was conducted using an LGR liquid water isotope analyzer (LWIA-24d).

4. Results

4.1. Bedrock structure

4.1.1. Maimai M8 bedrock structure

The conglomerate at M8 had characteristics that resembled saprolite or regolith more than well cemented bedrock. Drill rates were as high as 0.5 m min^{-1} and core retrieval was poor, typically approximately 10% (i.e. for every 1 m drilled, 0.1 m of core was recovered). The sandy matrix was friable, eroded when drilled and produced very little core compared to more competent hard bedrock drilled at other sites as reported in Gabrielli and McDonnell (2011). These characteristics made it impossible to reconstruct an accurate well log based on sparse and sporadic core retrieval and observed drilling characteristics. Although some heterogeneity was detected during drilling (e.g. bedded layers of varying clast size), it was difficult to identify distinct stratification or fracturing with any degree of certainty. A visual inspection of 50 m^2 of open bedrock surface at the toe of the hillslope revealed no major fractures. Samples hand-excavated from the top 0.6 m of bedrock had oxidized surfaces at the clast–matrix boundary, indicating possible water circulation. We were unable to ascertain if the weathered surfaces existed further into the bedrock due to the erosive nature of the drilling process and minimal core recovery.

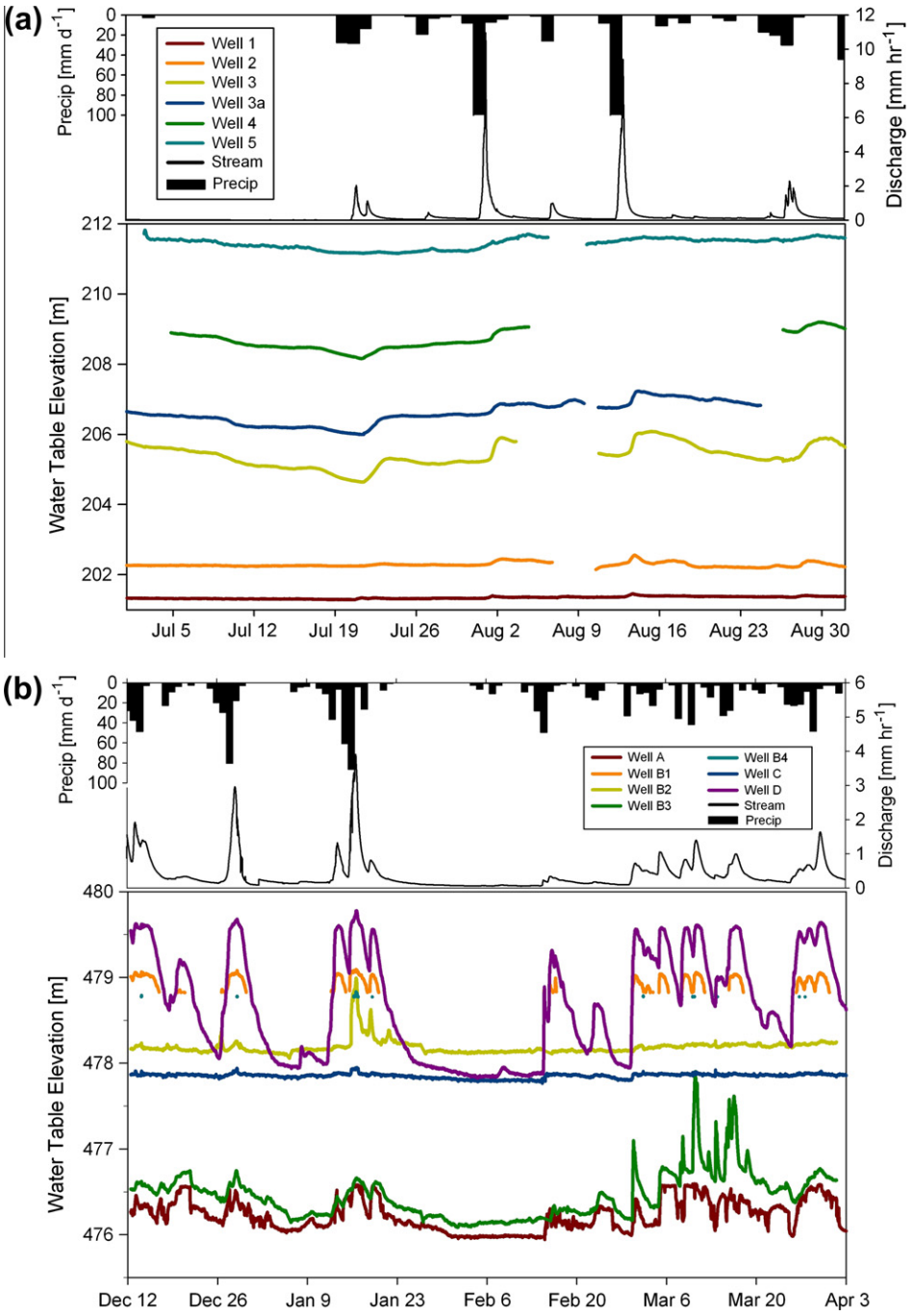

Fig. 3. Water table elevation data from bedrock wells at M8 (a) and WS10 (b) along with corresponding stream hydrograph and rainfall hyetograph.

Slug tests of each well in the M8 hillslope transect revealed decreasing hydraulic conductivity with distance upslope (Table 2). Although precise Ksat values were difficult to quantify with such small volume slug tests due to the narrow wells associated with our portable drill system and borehole storage effects, general order-of-magnitude values were achieved and offer insights to the spatial variation in bedrock characteristics from well to well across the hillslope. For instance, Well 1 at the toe of the hillslope had an apparent Ksat three orders of magnitude greater than Well 5, 30 m upslope.

Pump tests were also conducted on each well, however, due to insufficient pump rates or extremely slow recharge, the tests were unsuccessful in producing reliable values for transmissivity, hydraulic conductivity or storativity; however, relative hydrologic data were gained from these generalized tests. For instance, despite 60 min of pumping at a rate of 0.25 L min^{-1}, a volume equivalent to 10 times the borehole storage, the water table elevation at Well 1 remained constant suggesting an aquifer with considerable storage or high permeability. Pump rates could not be increased and therefore, the aquifer could not be stressed sufficiently to yield reliable drawdown or recharge tests. Wells 2–5, however, were also pumped t 0.25 L min^{-1} but were evacuated after only 5–10 min of pumping, suggesting a decrease in hydraulic conductivity with distance upslope (consistent with the slug test results). The bedrock samples cut from the free surface of the bedrock and measured in the lab for porosity had an average value of 25%

and are in the range of established general porosities for sandstone and packed gravel (Freeze and Cherry, 1979). Additionally, Ksat values <0.001 and >1 mm d^{-1} measured through slug tests (Table 2) agree to within an order of magnitude of values measured by Graham et al. (2010b).

4.1.2. H.J. Andrews WS10 bedrock structure

Maximum drill rates through the tuff and breccias at WS10 was 0.1 m min^{-1} (5× slower than at M8), but core recovery was nearly 95% for all wells. The high core recovery and the use of a down-the-hole camera provided detailed stratigraphic data and direct observation of the permeability architecture of the bedrock underlying WS10. The bedrock displayed two distinct horizons: a highly-fractured, weathered layer approximately one meter thick and less weathered rock with discrete fractures and occasional deeper facture zones. Fracture density in the upper layer approached 18–29 fractures per meter, while deeper regions contained fracture densities of only 4–9 fractures per meter. Most fractures and fracture zones were oriented between horizontal and 45°. Occasional isolated fractures were oriented at steep dips ranging from 60° to 90°, sometimes connecting the shallow dipping fracture zones. Most fracture planes were stained by iron oxide, more than likely associated with transient water circulation. Additionally, water was noted discharging from some fractures during borehole videoing, even during low flow summer periods.

Pump tests were attempted in some of the boreholes at WS10; however, most boreholes pumped dry after only 5–10 min at discharge of rates of <0.1 l min^{-1}, indicating minimal storage or low permeability in the surrounding bedrock.

4.2. Groundwater dynamics

4.2.1. Maimai M8 groundwater dynamics

Ten storm events with precipitation totals greater than 8 mm were recorded during the study period. Twenty-four hour precipitation totals ranged from 1 to 129 mm, with a 1-h maximum rainfall intensity of 15 mm occurring during the August 1 event. Stream discharge ranged from a low of 0.007 mm h^{-1} during a 3 week dry period to a maximum of 10.9 mm h^{-1} during the August 1 event. Fig. 3a shows the time series data of bedrock water table elevations, the hydrograph and the hyetograph during the study period.

Fig. 2a displays water table dynamics in each well in the context of well location on the hillslope. All wells contained water during the study period except for Well 5, which dried during a 3 week period in mid-June. Depth to water table increased with distance upslope. At Well 1, the toe of the hillslope, the water table was located approximately 1.7 m below the SBI, while approximately 30 m upslope at Well 5, the water table was located 4.7 m below the SBI.

All wells showed a change in water level that correlated well to precipitation events. The amplitude of this response varied spatially across the hillslope. Table 2 includes the water table increase per millimeter of rain averaged across all storm events greater than 8 mm total precipitation for each well. Wells 1 and 2 had the smallest water table fluctuations during storm events with total changes of only 0.08 m and 0.17 m for Wells 1 and 2, respectively. The amplitude of water table fluctuation increased with distance upslope for Wells 3, 3a and 4, despite the depth to water table increasing into the bedrock. Well 3 had the largest response to a storm event with a change in water table elevation of 0.67 m during the August 1 rainfall event. As distance increased upslope, water table response began to decline and Well 5 showed decreased response to storm events compared to the middle wells (3, 3a and 4).

Timing and rate of well response to storm events was investigated to characterize the basic dynamics of water table fluctuations, as well as to identify spatial patterns within the hillslope and possible correlations between the timing of stream discharge and well fluctuations. The time lag from initiation of precipitation to initiation of well response increased with distance upslope. Wells lower in the hillslope responded quickly (60–100 min) to the onset of precipitation, and also had the greatest rate of increase in water table, often tracking identically with the sharp rise and recession of the stream hydrograph. Fig. 4 shows the time series of water table dynamics for Well 1 and highlights the minimal water table fluctuations but the rapid storm response and coincident nature of the response of bedrock groundwater in Well 1 and the catchment discharge. Water table response became more attenuated and delayed with distance upslope, although the middle wells (3, 3a and 4) still responded on the time scale of the storm event. At the upper end of the transect, water table dynamics in Well 5 were very damped and attenuated, having storm responses that occurred across multiple day time periods.

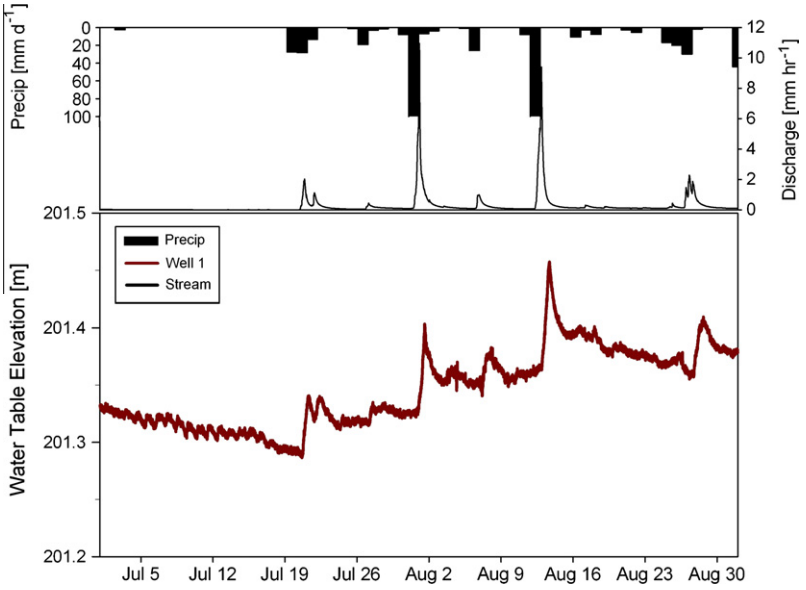

Fig. 4. Water table elevation data from bedrock well 1 at M8 showing a close up of the water table dynamics that is not visible at the larger scale of Fig. 3.

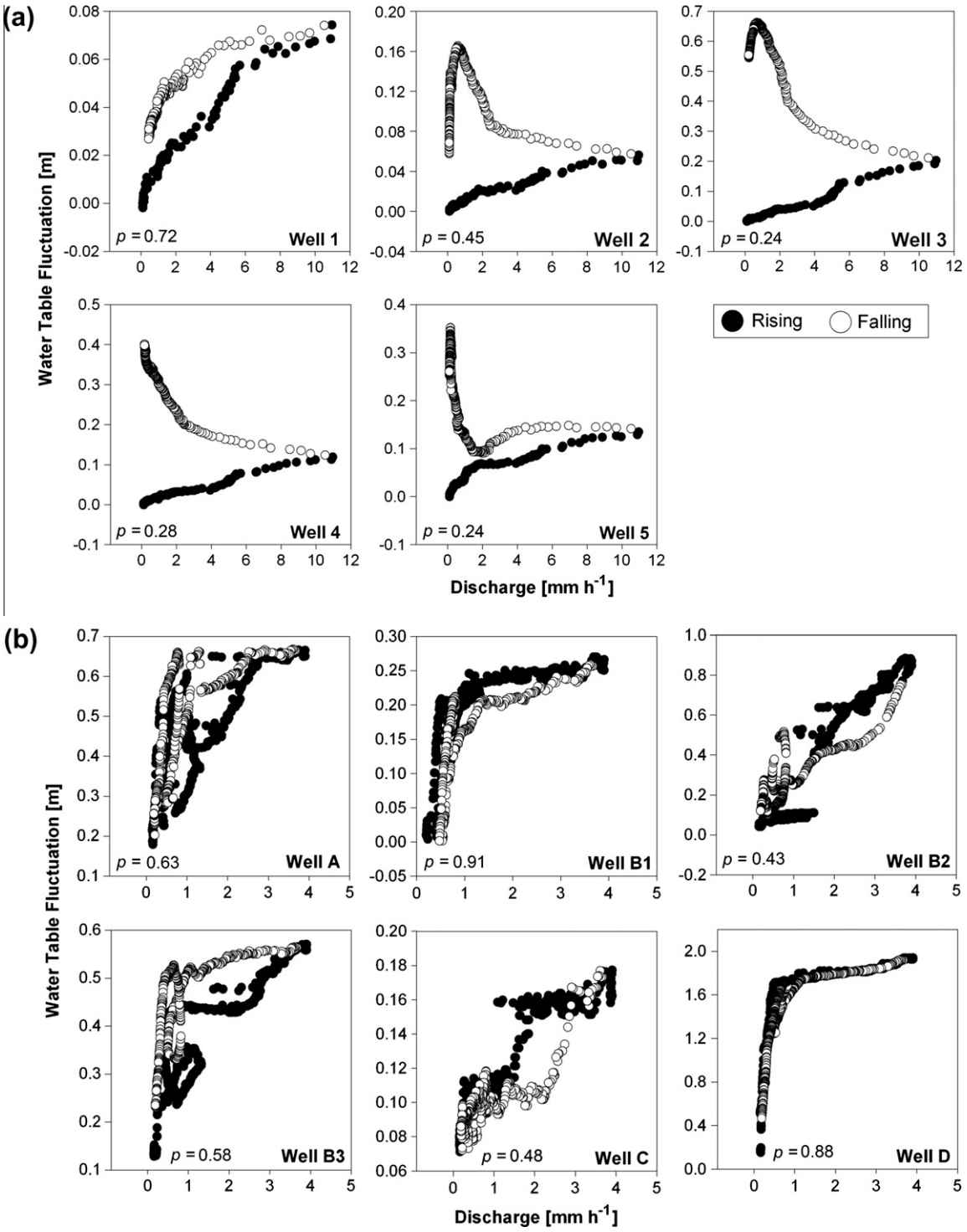

Fig. 5. Relationship between runoff and change in water table for each well during the August 2 storm event at M8 (a) and the December 28 storm event at WS10 (b). The Spearman's rank correlation coefficient (ρ) is displayed for each well.

Fig. 5a shows the relationship between the storm hydrograph and water table elevations in each of the wells. All wells showed an anti-clockwise hysteretic relation with streamflow, implying the near stream groundwater led the rising limb of the hydrograph, while the deeper bedrock groundwater farther upslope controlled the stream hydrograph falling limb. Spearman's rank correlation coefficient was calculated for these data (Table 2). This non-parameterized measure of statistical dependence measures the correlation between changes in the storm hydrograph and changes in water tables within each well, while also accounting for different relationships (e.g. linear, logarithmic, etc.) that may exist between the well fluctuations and the storm hydrograph (Seibert et al., 2003). Well 1 had the strongest correlation to the storm hydrograph, and although changes in the water table elevation were minimal (<0.08 m), they followed closely with stream fluctuations despite being over 15 m from the stream channel. The correlation between well fluctuations and the storm hydrograph weakened with distance upslope, as

expected by the increasingly delayed and attenuated storm response.

4.2.2. H.J. Andrews WS10 groundwater dynamics

Sixteen storm events with precipitation totals greater than 8 mm were recorded during the study period. Twenty-four hour precipitation totals ranged from 1 mm to 86 mm, with a 1-h maximum rainfall intensity of 12 mm occurring during the February 15 event. Stream discharge ranged from a dry season low of 0.05 mm h^{-1} to a maximum of 3.9 mm h^{-1} during the January 16 event. Fig. 3 shows the time series data of bedrock water table elevations, the hydrograph and the hyetograph during the study period.

The bedrock groundwater dynamics at WS10 displayed an array of different characteristics depending on well depth, well location and intersection with conductive fracture zones. Table 2 shows the general hydrometric characteristics of the wells and Fig. 2b shows the well dynamics in context to their location on the hillslope. All wells retained some water during the study period except for the two shallow wells, B1 and B4, that wetted up only during storm events. Depth to water table and water table dynamics were influenced by the heterogeneity of the fracture network within the bedrock and, unlike the hillslope at M8, no pattern was observed with distance upslope.

Two bedrock horizons displayed distinct water table responses. The upper layer consisting of highly fractured, highly transmissive bedrock had measurable water tables only during storm events (Wells B1 and B4) and the deeper zone that remained permanently wet throughout the study period. Wells penetrating into the deeper zone had water tables that either fluctuated considerably during events (Wells A, B3 and D) or showed little or no response through the entire study period (Wells B2 and C).

Wells B1 and B4 only became active during storm events, and further, only became active when the water table elevation in Well D (upslope) reached a critical level. The drilling log for Well D showed a major fracture zone at this critical point (~1.7 m below the SBI) and we hypothesize that the water table rises up to this fracture zone in Well D and then spills over, initiating subsurface lateral flow through the bedrock that then initiates a water table response in Wells B1 and B4. Well logs for Wells B1 and B4 showed hydrologically active fractures located just 0.3 m into the bedrock, indicating that the fracture zone connecting upslope Well D to downslope wells B1 and B4 gets shallower with distance downslope. Additionally, during installation of wells B1 and B4, drilling fluid (the silt laden water produced while drilling) was observed draining into this fracture pathway and then reemerging downslope in the hillslope trench, suggesting that this hydrologically active fracture zone initiates upslope of Well D, travels downslope through Wells B1 and B4 and pinches out at the soil bedrock interface above the trench. Further, during storm events the water table in Well D would rise rapidly to the level of the fracture zone and then plateau with little or no further water table increase. This process, similar to transmissivity feedback in till mantled terrain (Bishop, 1991), creates a visual capping effect in the water table time series (Fig. 3b) and was also noted in Well A suggesting the occurrence of significant subsurface lateral flow through the bedrock.

Well C remained wet for the duration of the study period, yet there was little or no response in the water table elevation and no long-term variations were observed through the duration of monitoring despite being located only 4 m from Well D which responded rapidly to storm events and had water table fluctuations of up to 1.6 m. Additionally, the water table in Well C recovered quickly proceeding a 30 min pumping test that removed a volume of water equivalent to three times the borehole storage. It is likely that the bedrock aquifer accessed by Well C is compartmentalized and isolated from the local hillslope processes that occur on a storm-event time scale.

Wells A and B3 had similar water table elevations and similar water table dynamics during storm events, likely denoting the intersection of the same fracture zone by each well. Well B3 had slightly higher water table elevations indicating a downslope gradient towards Well A, and the water table in both of these wells remained above the elevation of the stream channel denoting a gaining reach in the stream.

Fig. 5b shows the relationship between the storm hydrograph and water table elevations in each of the wells. A threshold relationship appears to exist between many bedrock wells and the stream discharge. Water tables in the bedrock rise sharply to a threshold level prior to stream response, then stream response occurs with little additional rise in the bedrock water tables suggesting a fill and spill mechanism. Spearman's rank correlation coefficients were also computed for each well and results are shown in Table 2. Although some wells were more correlated with fluctuations in catchment discharge than others, there was no discernible spatial pattern to the connectivity. The heterogeneity of the fracture network within the hillslope bedrock explains this lack of correlation.

4.3. Bedrock groundwater contributions to hillslope discharge

Our main approach in determining whether bedrock groundwater contributed to hillslope discharge was to identify whether water tables rose to or above the soil–bedrock interface. It was assumed that direct contribution of bedrock groundwater to hillslope runoff would occur if water tables within the bedrock rose into the highly transmissive soil mantle. Monitoring through a range of storm event sizes and antecedent conditions provided a strong test of this hypothesis. Additionally, we asked whether bedrock groundwater was isotopically distinct from streamflow and hillslope trench water, providing supporting evidence to back-up or refute our hydrometric interpretation for groundwater contributions. It was assumed that if bedrock groundwater rose above the SBI and contributed materially to hillslope runoff, then the isotopic signature of the hillslope discharge (trenchflow) would show evidence of bedrock groundwater mixing.

4.3.1. Bedrock groundwater contributions at Maimai M8

Water tables in the wells measuring bedrock groundwater in the M8 hillslope never rose to or above the soil–bedrock interface and thus, did not contribute directly to subsurface lateral flow from the hillslope. Well 1, located 15 m from the stream channel, had a water table closest to the soil bedrock interface.

Isotope sampling of the rainfall, boreholes, hillslope trenchflow and stream support the well-based hydrometric evidence of little event-based mixing between the bedrock groundwater and subsurface stormflow compartments. Isotope data collected during a 36 mm storm event is shown in Fig. 6a and descriptive statistics of the observed isotope signals are provided in Table 3. The isotopic signature of the bedrock groundwater collected from Wells 1, 2, 3 and 5 was distinct from that of the stream water and trench water (soil). The stream water shifted toward the heavier (more positive) isotopic signatures of the trench and rain water during the peak of the storm and then became lighter (more negative) after the storm peaked. The bedrock groundwater had a lighter isotopic signature than the stream and the trench (soil) water, and remained relatively unchanged through the duration of the event and well past the storm recession. The steady isotopic signature of the bedrock groundwater and the deflection of the trenchflow isotopic signature away from the storm event suggest there is no direct contribution of bedrock groundwater to hillslope discharge.

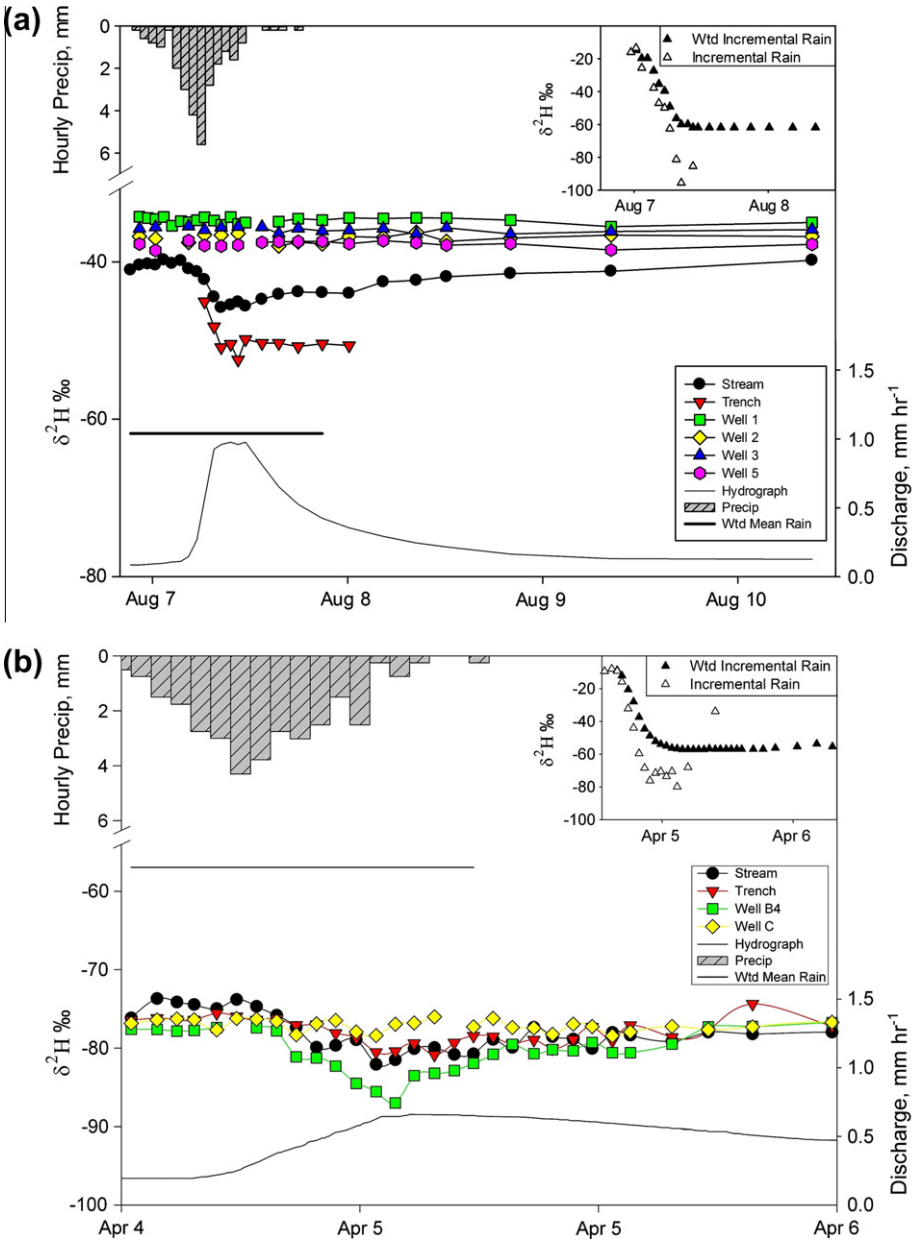

Fig. 6. Stable isotope time series data for sampled storm event at M8 (a) and WS10 (b) with hydrograph and hyetograph. Total storm precipitation was 36 mm at M8 and 34 mm at WS10. The horizontal black line represents total storm weighted mean rain deuterium value. The inset diagrams in each plot display the isotopic values of the high frequency sequential samples of rain water (with each dot representing a point sample taken at hourly increments) in the solid triangles and the calculated incremental mean of the time series during the storm progression shown in the open triangles. Isotope values for some wells at WS10 (b) were not displayed for visual clarity. Those wells are discussed in the text. Wells that accessed deeper bedrock groundwater followed similar trends as Well C, while shallow bedrock wells followed the trend of Well B4.

4.3.2. Bedrock groundwater contributions at H.J. Andrews WS10

Water tables within the wells measuring bedrock groundwater in the WS10 hillslope never rose to or above the soil–bedrock interface. The water table in Well B4 was nearest the surface, but never rose higher than 0.3 m into the bedrock. Fig. 6b shows the times series of isotope analysis during a 34 mm storm event and Table 3 provides descriptive statistics of the observed isotope signals. Here again, isotope sampling of the rainfall, boreholes, hillslope trenchflow and stream support the well-based hydrometric evidence of little event-based mixing between subsurface stormflow compartments. Isotope values in the wells showed two distinct responses: Well C, accessing deeper compartments, had minimal deflection towards that of rainfall or trenchflow supporting the claim that the water table does not rise above the SBI and contribute directly to hillslope discharge. Shallow Well B4, however, shifted towards a lighter (more negative) isotopic signature similar to the storm-based deflections of the trenchflow and stream discharge, indicating the addition of a similar isotopically lighter component to the shallow fractured bedrock, the hillslope runoff, and the stream discharge. Although this isotopically lighter component was not captured by the end member samples of rainfall, trenchflow and groundwater, we speculate that unsampled vadose zone water is the likely missing end member. Once the storm peak passed and the recession

Table 3
Descriptive statistics of observed isotope signals.

Sample location	Min.	Max.	Average[a]
Maimai			
Stream	−45.8	−39.8	−42.4 ± 2.0
Trench	−52.4	−45.0	−49.9 ± 1.9
Precip.	−95.6	−13.5	−51.5 ± 29.2
Well 1	−35.5	−34.3	−34.7 ± 0.4
Well 2	−38.0	−36.2	−37.0 ± 0.5
Well 3	−36.8	−35.5	−35.9 ± 0.4
Well 5	−38.5	−37.3	−37.7 ± 0.4
WS10			
Stream	−82.1	−73.7	−77.9 ± 2.3
Trench	−83.5	−74.7	−78.5 ± 2.5
Precip	−79.9	−7.9	−49.4 ± 27.1
Well B4	−87.0	−76.5	−80.0 ± 2.8
Well C	−78.4	−76.0	−77.2 ± 0.7

[a] Sample count varied between sample location. Average includes ±1 standard deviation.

began, the isotope composition of the stream, trench and wells shifted back to similar values.

5. Discussion

5.1. An evolving perceptual model of hillslope hydrology at two benchmark sites

While a number of studies have addressed the influence of bedrock structure on catchment processes through indirect (i.e. spring or seepage analysis (Iwagami et al., 2010)) and direct measurements at single sites (Banks et al., 2009; Haria and Shand, 2004; Kosugi et al., 2008; Montgomery et al., 1997; Uchida et al., 2002; Wilson and Dietrich, 1987), we know of no studies that have compared hillslope and catchment-scale runoff processes through comparative analysis of directly monitored bedrock groundwater dynamics and core-based bedrock structure at previous benchmark hillslope hydrological sites. Our study, therefore, affords the ability to further the evolving perceptual model of hillslope hydrology at Maimai and H.J. Andrews. We do this below by contributing new insights on the role of bedrock groundwater to the already rich understanding of soil mantle subsurface stormflow processes established in previous papers by different groups working at both sites.

5.1.1. Maimai M8

Early work by Mosley (1979), Pearce et al. (1986), Sklash et al. (1986) and McDonnell (1990) shaped the understanding of runoff behavior at Maimai, through iterative study of subsurface stormflow mechanisms, with different approaches and different interpretations. Despite over 30 years of work dedicated to this single site, studies still emerge from this catchment with new perceptual models of how runoff is formed at the hillslope and catchment scales (Graham et al., 2010b; McGlynn et al., 2004). To date, the bedrock at Maimai has been described as "poorly permeable" (O'Loughlin et al., 2002, p. 2), "effectively impermeable" (McDonnell, 1990, p. 1), and "impermeable" (McGlynn et al., 2002, p. 23), despite the fact that no direct measurements were taken of its hydraulic conductivity or permeability. Graham et al. (2010b) challenged this perception with measured Ksat of 1–3 mm h^{-1}; a value that suggests that bedrock groundwater could exert influence on storm runoff.

Our observations of event-based bedrock groundwater response to storm rainfall shows three distinct zones of behavior: a lower, middle and upper region that responds differently due to differing bedrock properties and depth to water tables. The lower section nearest the stream is defined by a water table response that is small in magnitude but rapid and coincident to the catchment discharge response. The higher hydraulic conductivity of this region, as shown by our slug tests, is able to accommodate greater flow through the bedrock without major increases in water table elevations, and thus the magnitude of the water table response is small. Despite the minimal fluctuations in the water table, the response is rapid and highly correlated to catchment discharge (Fig. 4). The shallow depth to the water table may allow the storm signal to move rapidly through the bedrock, and additionally, McGlynn et al. (2004) showed a strong correlation between riparian zone groundwater levels and runoff for the headwater catchments at Maimai. This, along with the high Spearman rank correlation coefficient between Well 1 and the stream, suggest that these regions may be tightly coupled with each other explaining the rapid storm response in the in this lower region of the hillslope.

Farther upslope (Wells 3, 3a, and 4), groundwater dynamics lose their correlation to the storm hydrograph and become more delayed and attenuated, while also having considerably larger fluctuations in water table elevations. The lower hydraulic conductivity in this region is unable to permit circulation hydraulically down gradient as rapidly, and thus the water table rise is greater in response to storm events than in the lower hillslope region. The water table in this region of the hillslope, however, is still close enough to the bedrock surface that responses occur on a storm-event time scale. With additional distance upslope (Well 5), the water table is deep enough into the bedrock (~5 m) and the hydraulic conductivity low enough that the storm signal becomes even more attenuated and delayed (on the order of days), thus removing any correlation between water table fluctuations and the stream hydrograph. Further, there exists some anomalous behavior of water table fluctuations within Well 5 that are difficult to explain with respect to rainfall input (e.g. water table increase prior to the August 2 storm event). One might suspect a faulty seal at the soil–bedrock interface allowing event water moving vertically down the well annulus to contaminate the groundwater signal; however, we have isotope analysis during a storm event showing no deviation of water composition. An alternative hypothesis to explain these data may be changes in barometric pressure. Such changes are capable of producing considerable hydrologic response in water table elevations within wells (Rasmussen and Crawford, 1997), and it appears that our observed rise in water table prior to the onset of the storm event precipitation may be a function of the barometric efficiency of the aquifer.

Graham et al. (2010b) showed that the surface bedrock had a hydraulic conductivity high enough to account annually for >1000 mm of water balance loss annually into the bedrock. Old Man Gravel as a bedrock unit is comparatively soft, weathered, and loosely consolidated. The friable sandy matrix is easily crumbled by hand and holds little structural capacity, lending it to a description more similar to saprolite or regolith than competent hard rock. Perhaps the best local proxy for our hydrogeological situation is the Moutere Gravel groundwater system that exists north-east of the Old Man Gravel. The Moutere Gravel is comprised primarily of sandstone clasts in a clay-bound muddy sand matrix (Stewart and Thomas, 2002). The principal mechanism of groundwater recharge to shallow aquifers has been identified as direct rainfall infiltration through unconfined regions, consistent with our limited measurements at Maimai.

Fig. 7a illustrates our new perceptual model of contributions to hillslope and catchment flow at M8. This current study has shown the bedrock to be quite permeable with a structure that promotes bulk water flow and significant storm response in the bedrock aquifer. For the storms monitored, bedrock groundwater did not rise above the soil bedrock interface, and therefore, did not contribute directly to the subsurface lateral stormflow. This interpretation

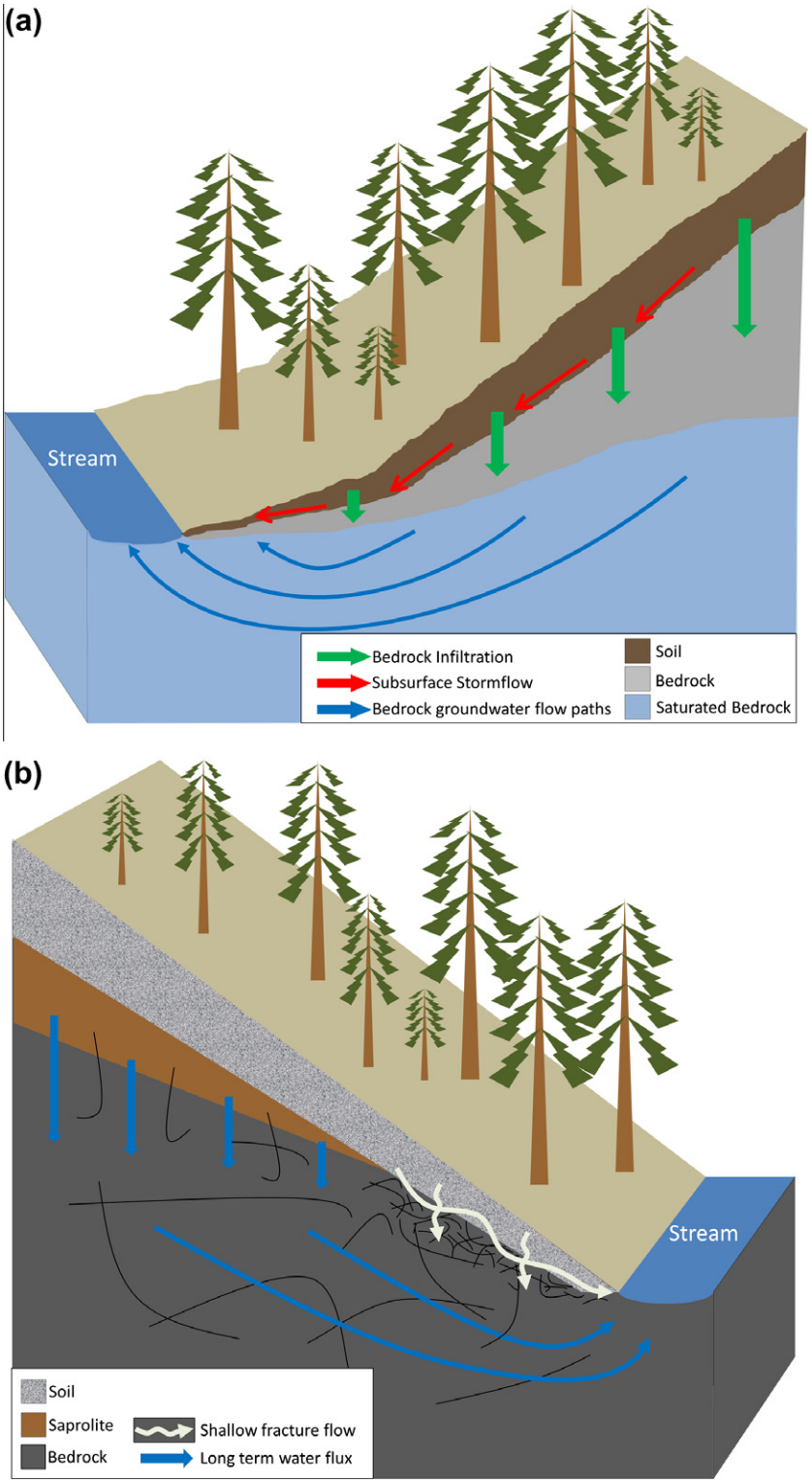

Fig. 7. Perceptual models of water flow through (a) M8 hillslope and (b) WS10 hillslope. The M8 model highlights significant seepage into the bedrock that ultimately re-emerges at the stream channel, while the WS10 model shows movement of water through fracture pathways resulting in lateral subsurface stormflow in the shallow highly fractured bedrock and deeper seepage returning as baseflow through longer more tortuous flow paths in the deeper less fractured bedrock.

was supported by isotopic evidence showing no deflection in the isotopic signature of bedrock groundwater towards either the soil water (trench water) or precipitation values during a storm event, implying no mixing within the bedrock on the event time frame. Nevertheless, the dynamic response of bedrock water tables on a storm-event time scale (Fig. 3a) offers evidence of bedrock groundwater responsiveness and potential significance at the catchment scale. Indeed if one examines the runoff ratios at the hillslope and catchment scales at Maimai, reported M8 hillslope runoff ratios are on the order of 13% (Woods and Rowe, 1996), while the catchment wide runoff ratio is nearly 60% (Woods and Rowe, 1996). This strong dichotomy suggests that groundwater likely

influences stream response independent of shallow, lateral flow paths that have been the focus of so many previous studies at the site (as reviewed by McGlynn et al. (2002)).

5.1.2. H.J. Andrews WS10

Watershed 10 at the H.J. Andrews, like M8 at Maimai, has been the site of a significant number of influential studies that have shaped the understanding of hillslope hydrology in steep, humid catchments. Harr's (1977) seminal work shed light on the processes of subsurface stormflow, near stream saturated zones, and transient saturation at the soil–bedrock interface. Harr found that only the region within the first 12–15 m of the stream channel became saturated (at the soil–bedrock interface) during storm events, while upslope regions had transient saturated patches where fluxes were high (i.e. 10–25 cm h^{-1}) if connected to the near-stream saturated zone. More recently, McGuire and McDonnell (2010) investigated hillslope–stream connectivity in this same catchment and found that far upslope areas contributed directly to subsurface runoff from the hillslope, implying the existence of preferential flow paths that short circuit traditional matrix flow through the soil. Our current work offers further evidence regarding the nature of the transient saturated zones and provides evidence for additional high flux pathways within the bedrock that are capable of connecting upslope with downslope regions and eventually with the stream channel.

Fig. 7b illustrates our new perceptual model of contributions to hillslope and catchment flow at WS10. Our findings suggest that the bedrock groundwater table does not rise above the soil–bedrock interface and thus, does not contribute directly to lateral subsurface stormflow at the soil bedrock interface. We do have evidence, however, that the very shallow highly fractured bedrock in and around the soil–bedrock interface does exert an influence on runoff processes and contributes directly to lateral subsurface stormflow. We hypothesize that once subsurface stormflow occurs, some portion of the flow is lost as seepage to the fractured bedrock. Once in the bedrock, circulation is controlled by the fracture network density, geometry and connectivity (Banks et al., 2009) and is extremely heterogeneous. Well dynamics shown in Fig. 3b provides evidence of differing flow paths within the fractured bedrock as the water table response between wells are highly variable despite their close proximity. Some flow follows deeper fracture pathways connecting to a deeper bedrock aquifer. This seepage does not play a direct role in the storm event runoff, but instead follows classic groundwater discharge pathways that maintain baseflow conditions (Winter, 2007). Subsurface stormflow that follows shallow bedrock fracture pathways may either remerge at the soil bedrock interface if the fracture pinches out, or may directly bypass to the stream channel depending on the fracture network. In both cases, this water has a direct contribution to storm runoff. Graham et al. (2010a) showed that near surface fractured bedrock constituted a significant flow path in the WS10 hillslope, nearly equal in volume to subsurface lateral flow in the soil during a sprinkler experiment that brought the WS10 instrumented hillslope up to steady state discharge. Highly fractured regions of bedrock can act to either prevent saturation due to highly transmissive fractures that transport water rapidly downslope, or augment saturation at the soil bedrock interface by acting as an exfiltration zone which transports and concentrates water from upslope regions to downslope regions. Similar findings have been reported by others. For example, Uchida et al. (2002) determined that exfiltrating bedrock groundwater was an important contributor to transient groundwater in upper hillslope regions in a zero-order catchment in Central Japan. Wilson and Dietrich (1987) noted that bedrock return flow occurred where fractured bedrock encountered a competent zone that forced flow back up into the subsoil, creating a transient saturated zone. Montgomery et al. (2002) and Anderson et al. (1997) found that return flow from bedrock created zones of transient saturation at the soil bedrock interface, and deeper bedrock pathways carried tracers rapidly through the subsurface to the channel head.

Considering the heterogeneity of fractured bedrock, it is possible to conceive of a patchy network of saturated zones in upslope regions that are in part, controlled by the underlying bedrock. Saturated zones would occur on top of more competent regions, while unsaturated zone would occur over fractured regions. The hillslope would then display variably saturated conditions depending on rainfall amount, intensity, and antecedent conditions, similar to what both Harr (1977) and McGuire and McDonnell (2010) reported. The isotope time series (Fig. 6b) shows Well B4, the trench and the stream all shifting away from the rain input signal towards lighter isotopic values immediately prior to the hydrograph peak. Although we cannot directly identify the water source that is causing this shift (although we hypothesize that it is unmeasured soil water/vadose water end member), we are able to rule out event water as the source of water into the bedrock.

5.2. Similar hillslope forms can hide radically different plumbing

M8 and WS10 share strikingly similar catchment size, average slope angle, length and relief, soil properties, average yearly rainfall totals and catchment runoff ratios (see comparative watershed model analysis by Sayama and McDonnell (2009)). Both catchments are highly responsive (Harr, 1977; Mosley, 1979) and if viewed from their respective outlets the catchments appear to be nearly identical (Table 1). Despite these similarities, these catchments hide radically different underlying geologic composition and structure, and as such, their hillslopes store and transmit water through distinctly different mechanisms. Some indications of this have been apparent from previous work (Sayama and McDonnell, 2009); most notably the distribution of soil depths at the two sites: Maimai shows a strong catenary sequence of thin, coarse soils on the ridges grading into deep colluvial-filled hollows with clays and other fines (Mosley, 1979). WS 10 shows an almost reverse pattern whereby soil depths increase progressively from thin, permeable soils near the toe of the hillslope to >7 m soil and sub-soil depths at the ridge (Harr, 1977).

The M8 hillslope appears to lack the WS10 bedrock fracture flow paths, however, the permeable bedrock at M8 provides a greater potential for more spatially uniform recharge across the whole bedrock surface as infiltration would be possible everywhere below the soil mantle (although we know that there is considerable convergence of flow along the soil bedrock interface, as shown by the soil removal experiments of Graham et al. (2010b); hollows in particular may be enhanced zones of deep, groundwater recharge). Alternatively, at WS10, the dual porosity bedrock structure facilitates flow through only the fracture pathways on a storm-event time scale, as opposed to the intergranular pore space of the bedrock matrix as seen at Maimai. Infiltration into the bedrock would then be directly controlled by not only the spatial heterogeneity of fractures at the bedrock surface at WS10, but also by the heterogeneity and anisotropy of the fracture properties deeper in the bedrock, such as density, connectedness, and aperture size.

Comparing catchment versus hillslope runoff at each site reveals how these different structural geologies affect the hillslope and catchment flow regimes. As stated earlier, Woods and Rowe (1996) reported M8 hillslope runoff ratios of only 13%, while the catchment wide runoff ratio is nearly 60%. Aside from rainfall landing directly on the riparian zone and stream channel and assuming no interbasin transfer, this difference (47% minus stream and riparian interception) would likely be caused by water seeping into the hillslope bedrock (as shown elsewhere with direct experiments; Tromp-van Meerveld et al. (2007), Graham et al. (2010b)). It is

assumed that this loss to bedrock bypasses colluvial hillslope processes and discharges directly into the stream channel or riparian zone, circumventing the trench installed at the hillslope–riparian interface, resulting in the low measured hillslope runoff. Our findings are consistent with Graham et al. (2010b) who calculated a loss to bedrock at the hillslope scale of 41% of rainfall at M8, and also concluded that flow reemerged into the stream channel through deeper bedrock pathways supporting this claim.

Runoff ratios at WS10 are approximately 56% of annual rainfall at the catchment scale (McGuire et al., 2005) and approximately 80% at the hillslope scale (calculated from rainfall and hillslope discharge during the 2010–2011 wet season). The high hillslope runoff ratio is indicative of a hillslope that sheds the majority of its water into the stream channel with little loss to deeper bedrock seepage. Graham et al. (2010a) calculated this deep seepage to be approximately 21% of precipitation during a sprinkler experiment that brought the WS10 hillslope up to steady state discharge. Although our work shows that both the upper (~1 m) and lower (~5 m) layers of bedrock were both shown to be hydrologically active during storm events, we hypothesize that the active upper layer returns flow back to the soil bedrock interface upslope of the stream channel on a storm-event time scale, thus accounting for the high hillslope runoff ratios. Both of these findings, at Maimai and WS10, highlight the sensitivity of how one calculates and compares hillslope vs. catchment runoff ratios based on trench placement. If the WS10 trench was located some meters upslope of its current position and likely capturing hillslope discharge without the deeper return flow, then the runoff ratio may have been more similar to that of the catchment. Alternatively, if the Maimai trench was located farther downslope and in or adjacent to the riparian area, then the hillslope flow recorded could have been augmented by bedrock groundwater returns.

One other notable difference between the M8 and WS10 catchments is the stream water mean residence time. The M8 watershed has an isotope-computed mean residence time of about 4 months, as reported by Pearce et al. (1986). The WS10 stream water mean residence time is on the order of 1.2 years, based on work reported by McGuire et al. (2005). The two subsurface, bedrock groundwater flow regimes help explain these measured mean residence time differences. Stream water mean residence time is directly proportional to storage (i.e. an increase in storage results in an increase in mean residence time) and inversely proportional to flux (for review, see McGuire and McDonnell (2007)). Katsuyama et al. (2010) examined bedrock groundwater recharge/discharge dynamics at six nested catchments underlain by weathered granite and found bedrock permeability and bedrock groundwater dynamics to be a dominant control of mean residence time at each catchment. Specifically, they found that mean residence time decreased with increases in bedrock infiltration. Bedrock infiltration into our experimental hillslopes can be inferred from differences in runoff ratios between the hillslopes and their catchments (the greater the difference the larger the flux into the hillslope), and the storage capacity from the different bedrock structure at each hillslope (Graham et al., 2010a). The porous Old Man Gravel at M8 has greater storage but also much greater flux. This, combined with the constant wet Maimai precipitation regime (a storm ~3 days with little seasonality) causes a constant flushing of water through the bedrock resulting in a shorter catchment-wide mean residence time, despite water following longer deeper flow paths traditionally considered slower.

The fractured bedrock at WS10 has both minimal storage and minimal flux. This produces a system with extreme seasonality in residence time. During the wet season when the hillslope sheds the majority of the rainfall input, runoff is high and residence time is low. During the dry season when baseflow constitutes the majority of runoff, the residence time is long as this water has traveled through longer, deeper, and more tortuous flow paths. Sayama and McDonnell (2009) showed that stream water mean residence time was largely influenced by the interactions between rainfall seasonality and soil mantle depth. We hypothesize that although greater volumes of younger-water discharge from WS10, the older water is disproportionately old due to extremely tortuous flow paths through deeper bedrock, resulting in a mean that is skewed towards longer timeframes. Our work, along with the work of Katsuyama et al. (2010), highlights the importance of understanding bedrock structure and its influence on flow paths within catchments and their imprint on mean residence time.

5.3. Next steps

Whether bedrock groundwater contributes directly to subsurface stormflow or indirectly, it is intimately connected to the processes involved with hillslope response and catchment runoff generation. Common themes are beginning to emerge from both previously well-monitored and well-documented sites and in new research locations, all demonstrating the importance of bedrock groundwater in different facets of the larger catchment hydrological cycle.

Variable flow sources in subsurface stormflow are controlled by transient saturation at the soil bedrock interface (McDonnell, 2003). The permeability of the underlying bedrock has been shown to affect the spatial and temporal development of these transient saturated zones in the soil mantle (Anderson et al., 1997; Haria and Shand, 2004; Hopp and McDonnell, 2009; Katsura et al., 2008; Katsuyama et al., 2005; Kosugi et al., 2008; Montgomery et al., 1997; Tromp-van Meerveld et al., 2007; Uchida et al., 2003, 2002; Wilson and Dietrich, 1987) as well as influence hillslope discharge into the riparian zone (Katsuyama et al., 2005), the overall catchment mean residence time (Katsuyama et al., 2010) the biogeochemistry of stormflow (Banks et al., 2009), and in some cases contribute considerably to storm runoff (Iwagami et al., 2010).

Our comparison of Maimai and WS10 revealed patterns and hydraulic behavior that could not otherwise have been identified through single hillslope analysis. The juxtaposition of similar catchment response despite wholly different geologies highlighted the fracture vs. bulk flow through the different systems. The implications of this work clearly demonstrate a shifting need for catchment hydrology to utilize structural geology, hydrogeology and bedrock well drilling to better understand the flow processes and hydrological functioning at hillslope and catchment scales. Site access continues to remain an issue, however, new technologies have been developed that offer light weight portable drilling systems capable of drilling bedrock in steep terrain inaccessible to normal drilling techniques (Gabrielli and McDonnell, 2011). Future work should exploit the dialog between experimentalist and modeler, where the complexities of bedrock flow, especially fracture flow can be explored within new model approaches (Kollet and Maxwell, 2006; Maxwell and Miller, 2005; Sudicky et al., 2008) that enable a holistic view of hillslope and catchment dynamics.

6. Conclusion

We examined the spatial and temporal dynamics of bedrock groundwater and its contribution to rainfall–runoff response at catchment and hillslope scales. The study was conducted at two previously well-studied sites, Watershed 10 at the H.J. Andrews in Oregon, USA and M8 at the Maimai in New Zealand. Boreholes were drilled into bedrock using a new drilling system designed by Gabrielli and McDonnell (2011). We did not reject our null hypothesis. Bedrock groundwater does not contribute directly to lateral subsurface stormflow within the soil mantle at either site.

We found no evidence of bedrock groundwater rising up into the soil mantle nor any control directly on subsurface flow generation at the soil–bedrock interface. Nevertheless, bedrock flow paths at WS10 in the shallow, highly fractured zone 1–2 m below the soil–bedrock interface was a key conduit for rapid lateral flow to the stream. However, this water was sourced primarily from a mix of vertically infiltrating soil water and rainwater into the upper bedrock zone and not from a rise water table from below. The bedrock structure of M8 was more permeable than previously thought, despite no evidence of surface fractures. Bulk water movement occurred primarily as seepage through the hillslope rather than as lateral subsurface stormflow along the soil–bedrock interface. Reemergence of hillslope bedrock groundwater appeared to occur in the riparian zone, resulting in a strong dichotomy between hillslope-scale and catchment-scale runoff ratios. The previously reported short mean residence time of stream water appears to be a function of the permeable bedrock and high storm intervals causing a steady flushing of water through the catchment.

We found a complex and highly fractured bedrock structure underlying the hillslope at WS10. Water movement through the bedrock was determined by the extent of the fracture network, its connectivity, and geometry. The highly fractured upper layer of bedrock acted as a lateral preferential flow path, connecting saturated upslope areas with near stream saturated zones. The deeper bedrock aquifer appeared to be recharged through discrete and isolated vertical fractures that connect to the surface. Although rainfall–runoff ratios were high for both the catchment and the hillslope, the mean residence time of stream water was four times older than the M8 catchment. We hypothesize that old bedrock groundwater from deeper pathways reemerges into the stream channel and skews the residence time towards older values despite being a small proportion, volumetrically, of the total stream discharge.

Acknowledgments

This work was supported through funding from NSF Grant NSF/DEB 0746179. We thank Ross Woods, John Payne, Iris Pitt, Travis Roth, Rosemary Fanelli and Tina Garland for help in the field and, Tim Burt, Keith Smettem, Cody Hale and Lyssette Munos Villers for useful discussions.

References

Anderson, S.P. et al., 1997. Subsurface flow paths in a steep, unchanneled catchment. Water Resour. Res. 33 (12), 2637–2653.
Bachmair, S., Weiler, M., 2011. New dimensions of hillslope hydrology forest hydrology and biogeochemistry. In: Levia, D.F., Carlyle-Moses, D., Tanaka, T. (Eds.), Ecological Studies. Springer, Netherlands, pp. 455–481.
Banks, E. et al., 2009. Fractured bedrock and saprolite hydrogeologic controls on groundwater/surface-water interaction: a conceptual model (Australia). Hydrogeol. J. 17 (8), 1969–1989.
Beven, K.J. (Ed.), 2006. Streamflow Generation Processes. Benchmark Papers in Hydrology, 1. International Association of Hydrological Sciences, Wallingford.
Bishop, K.H., 1991. Episodic Increase in Stream Acidity, Catchment Flow Pathways and Hydrograph Separation. Ph.D. Thesis, University of Cambridge, Cambridge, UK.
Bonell, M., 1998. Selected challenges in runoff generation research in forests from the hillslope to headwater drainage basin scale. J. Am. Water Resour. Assoc. 34 (4), 765–785.
Buttle, J. (Ed.), 1998. Fundamentals of Small Catchment Hydrology. Isotope Tracers in Catchment Hydrology. Elsevier, Amsterdam, pp. 1–43.
Dagan, G., 1978. A note on packer, slug, and recovery tests in unconfined aquifers. Water Resour. Res. 14 (5), 929–934.
Dietrich, P., Helmig, R., Sauter, M., Hötzl, H., Köngeter, J., Teutsch, G. (Eds.), 2005. Flow and Transport in Fractured Porous Media. Springer-Verlag, Berlin.
Dunne, T. (Ed.), 1978. Field Studies of Hillslope Flow Processes. Hillslope Hydrology. Wiley, Chichester, pp. 227–293.
Freeze, R.A., Cherry, J.A., 1979. Groundwater. Prentice-Hall, Inc., Englewood Cliffs, New Jersey.
Gabrielli, C.P., McDonnell, J.J., 2011. An inexpensive and portable drill rig for bedrock groundwater studies in headwater catchments. Hydrol. Process.
Graham, C.B., McDonnell, J.J., 2010. Hillslope threshold response to rainfall: (2) development and use of a macroscale model. J. Hydrol. 393 (1–2), 77–93.
Graham, C.B., Van Verseveld, W., Barnard, H.R., McDonnell, J.J., 2010a. Estimating the deep seepage component of the hillslope and catchment water balance within a measurement uncertainty framework. Hydrol. Process. 24 (25), 3631–3647.
Graham, C.B., Woods, R.A., McDonnell, J.J., 2010b. Hillslope threshold response to rainfall: (1) a field based forensic approach. J. Hydrol. 393 (1–2), 65–76.
Haria, A.H., Shand, P., 2004. Evidence for deep sub-surface flow routing in forested upland wales: implications for contaminant transport and stream flow generation. Hydrol. Earth Syst. Sci.
Harr, R.D., 1977. Water flux in soil and subsoil on a steep forested slope. J. Hydrol. 33 (1–2), 37–58.
Harr, R.D., McCorison, F.M., 1979. Initial effects of clearcut logging on size and timing of peak flows in a small watershed in western Oregon. Water Resour. Res. 15 (1), 90–94.
Harr, R.D., Ranken, D.W., 1972. Movement of Water through Forested Soils in Steep Topography. University of Washington, Seattle.
Hewlett, J., Hibbert, A., 1967. Factors affecting the response of small watersheds to precipitation in humid areas. In: Sopper, W.E., Lull, H.W. (Eds.), Proc. Int. Symp. on Forest Hydrology. Pergamon Press, Oxford, pp. 275–290.
Hopp, L., McDonnell, J.J., 2009. Connectivity at the hillslope scale: identifying interactions between storm size, bedrock permeability, slope angle and soil depth. J. Hydrol. 376 (3–4), 378–391.
Hursh, C., 1936. Storm-water and adsorption. Eos Trans. AGU 17, 301–302.
Iwagami, S., Tsujimura, M., Onda, Y., Shimada, J., Tanaka, T., 2010. Role of bedrock groundwater in the rainfall–runoff process in a small headwater catchment underlain by volcanic rock. Hydrol. Process. 24 (19), 2771–2783.
James, M., 1977. Rock Weathering in the Central Western Cascades. Thesis. University of Oregon, Eugene, OR, USA.
Katsura, S.Y., Kosugi, K.I., Mizutani, T., Okunaka, S., Mizuyama, T., 2008. Effects of bedrock groundwater on spatial and temporal variations in soil mantle groundwater in a steep granitic headwater catchment. Water Resour. Res. 44 (9), W09430.
Katsuyama, M., Ohte, N., Kabeya, N., 2005. Effects of bedrock permeability on hillslope and riparian groundwater dynamics in a weathered granite catchment. Water Resour. Res. 41 (1), W01010.
Katsuyama, M., Tani, M., Nishimoto, S., 2010. Connection between streamwater mean residence time and bedrock groundwater recharge/discharge dynamics in weathered granite catchments. Hydrol. Process. 24 (16), 2287–2299.
Kollet, S.J., Maxwell, R.M., 2006. Integrated surface–groundwater flow modeling: a free-surface overland flow boundary condition in a parallel groundwater flow model. Adv. Water Resour. 29 (7), 945–958.
Kosugi, K.I., Katsura, S.Y., Mizuyama, T., Okunaka, S., Mizutani, T., 2008. Anomalous behavior of soil mantle groundwater demonstrates the major effects of bedrock groundwater on surface hydrological processes. Water Resour. Res. 44 (1), W01407.
Maxwell, R.M., Miller, N.L., 2005. Development of a coupled land surface and groundwater model. J. Hydrometeorol. 6 (3), 233–247.
Mazurkiewicz, A.B., Callery, D.G., McDonnell, J.J., 2008. Assessing the controls of the snow energy balance and water available for runoff in a rain-on-snow environment. J. Hydrol. 354, 1–14.
McDonnell, J.J., 1990. A rationale for old water discharge through macropores in a steep, humid catchment. Water Resour. Res. 26 (11), 2821–2832.
McDonnell, J.J., 2003. Where does water go when it rains? Moving beyond the variable source area concept of rainfall–runoff response. Hydrol. Process. 17 (9), 1869–1875.
McDonnell, J.J. et al. (Eds.), 1998. Flow Pathways on Steep Forested Hillslopes: The Tracer, Tensiometer and Trough Approach. Environmental Forest Science. Kluwer Academic Publishers, pp. 463–474.
McDonnell, J.J., Tanaka, T., 2001. On the future of forest hydrology and biogeochemistry. Hydrol. Process. 15 (10), 2053–2055.
McGlynn, B.L., Mcdonnel, J.J., Brammer, D.D., 2002. A review of the evolving perceptual model of hillslope flowpaths at the maimai catchments, New Zealand. J. Hydrol. 257 (1–4), 1–26.
McGlynn, B.L., McDonnell, J.J., Seibert, J., Kendall, C., 2004. Scale effects on headwater catchment runoff timing, flow sources, and groundwater–streamflow relations. Water Resour. Res. 40 (7), W07504.
McGuire, K., McDonnell, J.J., 2007. Stable isotope tracers in watershed hydrology. In: Lajtha, K., Michener, W. (Eds.), Stable Isotopes in Ecology and Environmental Sciences, second ed. Blackwell Publishing, Oxford.
McGuire, K.J., McDonnell, J.J., 2010. Hydrological connectivity of hillslopes and streams: characteristic time scales and nonlinearities. Water Resour. Res. 46 (10), W10543.
McGuire, K.J. et al., 2005. The role of topography on catchment-scale water residence time. Water Resour. Res. 41 (5), W05002.
McGuire, K.J., Weiler, M., McDonnell, J.J., 2007. Integrating tracer experiments with modeling to assess runoff processes and water transit times. Adv. Water Resour. 30 (4), 824–837.
Montgomery, D.R., Dietrich, W.E., Heffner, J.T., 2002. Piezometric response in shallow bedrock at cb1: implications for runoff generation and landsliding. Water Resour. Res. 38 (12), 1274.
Montgomery, D.R. et al., 1997. Hydrologic response of a steep, unchanneled valley to natural and applied rainfall. Water Resour. Res. 33 (1), 91–109.
Mosley, M.P., 1979. Streamflow generation in a forested watershed, New Zealand. Water Resour. Res. 15 (4), 795–806.

O'loughlin, C.L., Rowe, L.K., Pearce, A.J., 2002. Sediment yields from small forested catchments, north Westland, New Zealand. J. Hydrol. (NZ) 17 (1), 1–15.
Onda, Y., Komatsu, Y., Tsujimura, M., Fujihara, J.-I., 2001. The role of subsurface runoff through bedrock on storm flow generation. Hydrol. Process. 15 (10), 1693–1706.
Pearce, A.J., Stewart, M.K., Sklash, M.G., 1986. Storm runoff generation in humid headwater catchments: 1. Where does the water come from? Water Resour. Res. 22 (8), 1263–1272.
Rasmussen, T.C., Crawford, L.A., 1997. Identifying and removing barometric pressure effects in confined and unconfined aquifers. Ground Water 35 (3), 502–511.
Rowe, L.K., Pearce, A.J., 1994. Hydrology and related changes after harvesting native forest catchments and establishing pinus radiata plantations. Part 2. The native forest water balance and changes in streamflow after harvesting. Hydrol. Process. 8 (4), 281–297.
Rowe, L.K., Pearce, A.J., O'loughlin, C.L., 1994. Hydrology and related changes after harvesting native forest catchments and establishing pinus radiata plantations. Part 1. Introduction to study. Hydrol. Process. 8 (3), 263–279.
Sayama, T., McDonnell, J.J., 2009. A new time-space accounting scheme to predict stream water residence time and hydrograph source components at the watershed scale. Water Resour. Res. 45 (7), W07401.
Seibert, J., Bishop, K., Rodhe, A., McDonnell, J.J., 2003. Groundwater dynamics along a hillslope: a test of the steady state hypothesis. Water Resour. Res. 39 (1), 1014.
Sklash, M.G., Stewart, M.K., Pearce, A.J., 1986. Storm runoff generation in humid headwater catchments: 2. A case study of hillslope and low-order stream response. Water Resour. Res. 22 (8), 1273–1282.
Sollins, P., Cromack, K., Mc Corison, F.M., Waring, R.H., Harr, R.D., 1980. Changes in nitrogen cycling at an old-growth douglas-fir site after disturbance. J. Environ. Qual. 10 (1), 37–42.
Sollins, P., Mccorison, F.M., 1981. Nitrogen and carbon solution chemistry of an old growth coniferous forest watershed before and after cutting. Water Resour. Res. 17 (5), 1409–1418.
Stewart, M., Thomas, J., 2002. Moutere Valley Groundwater: Nature and Recharge From Isotopes and Chemistry. Institute of Geological and Nuclear Sciences.
Sudicky, E., Jones, J., Park, Y.-J., Brookfield, A., Colautti, D., 2008. Simulating complex flow and transport dynamics in an integrated surface–subsurface modeling framework. Geosci. J. 12 (2), 107–122.
Swanson, F., James, M., 1975. Geology and Geomorphology of the H.J. Andrews Experimental Forest, Western Cascades, Oregon, Pac. Northwest For. and Range Exp. Stn., For. Serv., US Dept. of Agric., Portland, OR.
Triska, F.J., Sedell, J.R., Cromack, K.J., Gregory, S.V., Mccorison, F.M., 1984. Nitrogen budget for a small coniferous forest stream. Ecol. Monogr. 54 (1).
Tromp-Van Meerveld, H.J., Peters, N.E., McDonnell, J.J., 2007. Effect of bedrock permeability on subsurface stormflow and the water balance of a trenched hillslope at the Panola mountain research watershed, Georgia, USA. Hydrol. Process. 21 (6), 750–769.
Tsuboyama, Y., Sidle, R.C., Noguchi, S., Hosoda, I., 1994. Flow and solute transport through the soil matrix and macropores of a hillslope segment. Water Resour. Res. 30 (4), 879–890.
Uchida, T., Asano, Y., Ohte, N., Mizuyama, T., 2003. Seepage area and rate of bedrock groundwater discharge at a granitic unchanneled hillslope. Water Resour. Res. 39 (1), 1018.
Uchida, T., Kosugi, K.I., Mizuyama, T., 2002. Effects of pipe flow and bedrock groundwater on runoff generation in a steep headwater catchment in Ashiu, central Japan. Water Resour. Res. 38 (7), 1119.
Van Verseveld, W.J., McDonnell, J.J., Lajtha, K., 2009. The role of hillslope hydrology in controlling nutrient loss. J. Hydrol. 367 (3–4), 11.
Weiler, M., McDonnell, J.J., Tromp-Van Meerveld, I., Uchida, T., 2006. Subsurface Stormflow, Encyclopedia of Hydrological Sciences. John Wiley & Sons, Ltd.
Wilson, C.J., Dietrich, W.E., 1987. The Contribution of Bedrock Groundwater Flow to Storm Runoff and High Pore Pressure Development in Hollows, Erosion and Sedimentation in the Pacific Rim. IAHS, Corvallis, OR.
Winter, T.C., 2007. The role of ground water in generating streamflow in headwater areas and in maintaining base flow. J. Am. Water Resour. Assoc. 43 (1), 15–25.
Woods, R.A., Rowe, L., 1996. The changing spatial variability of subsurface flow across a hillside. J. Hydrol. (NZ) 35 (1), 49–84.